Revista Internacional de Métodos Numéricos para Cálculo y Diseño en Ingeniería

Construction monitoring and finite element simulation of assembly support for large cantilever cover beam

Chen Qu[1], Han Fang[1], Qingxing Feng[2]

1 School of Civil Engineering and Architecture, Zhejiang University of Science and Technology, Hangzhou 310023, Zhejiang, China

2 School of Civil Engineering and Architecture, Zhejiang University of Science and Technology, Hangzhou 310023, Zhejiang, China.

Abstract

The study on the assembly support for the large cantilevered cover beam was carried out by conducting real-time monitoring on the assembly frames' strain and displacement development processes in the actual project. Modeling of the support and numerical simulation for actual working conditions were presented. The monitoring data and analysis results show that the overall stress ratio of the support was less than 30%. And as the concrete structure being supported hardened, the support frame was unloaded. When the stress ratio was then reduced to less than 10%, it was the most appropriate time to remove the bracing frame. The maximum strain from the simulation did not exceed 66.26% of the theoretical maximum strain of the rod. The actual construction conditions and the spatial form of the support affected the force situation, resulting in the deviation from the theoretical maximum strain at certain phases. The analysis results and trends reflect the low utilisation rate of such framing rods. The results of the study can be used as a reference for the topology optimisation of assembled support frames for large cantilevered cover beams.

OPEN ACCESS

Published: 12/01/2023

Accepted: 26/12/2022

DOI: 10.23967/j.rimni.2023.01.001

Keywords:
Large cantilever fabricated support□Real time monitoring and early warning□Simulation analysis□Stress ratio utility analysis

1. Introduction

In the urban overpass system, it is common to see the existence of large cantilever poststressed cover beams for their overwhelming characteristics, such as long span, compactness, small footprint, openness to traffic and high rate of space utilization. Both local and oversea scholars have done in-depth studies on the full framing scaffolding due to its extensive use and the comprehensive construction technique [1-6]. With the development of industry, the demand for shortening construction time is increasing rapidly□as the traditional full framing scaffolding needs too much time and experienced workers to set up. Thus the large cantilever assembly support frame which will largely reduce the time and the flow period has become a better choice. With the open passages under, the influence on the local traffic can be minimized in the construction process. But so far, the focus in the previous researches about collapsible support frames has been more laid on the construction technology or shape design of frames, and less on the stress analysis of the support of the large cantilever cover beam. There are also researches simulating the loading conditions of some special form frames by the finite element analysis method, while less data in the actual construction process is available [7-11]. Moreover, there are researches on frame monitoring targeted for a particular construction case but not yet the study on real-time and full-range process monitoring [12-16].

This essay is based on the Hangzhou Pengbu Interchange Reconstruction Project. It focuses on the real-time information monitoring of the collapsible support frame for the large cantilever cover beam. In order to generate a comprehensive monitoring plan, the high-frequency acquisition instrument was used to monitor the whole actual process of construction all day in real-time. Through data analysis on the change of force in the different construction phases, this essay confirms the reliability of the support frame and proposes reference for its optimal flow. Furthermore, based on the results from the finite element simulation and monitoring data, the essay analysed about the main factors that may affect the stress conditions of the frame during the construction process. It provides technical support for safe construction and a basis for the broad application of this kind of support frame.

2. Project profile

The Hangzhou Pengbu Interchange Bridge Reconstruction Project is a reconstruction project at its original site. The total length of the route is around 1.73m. And the main highway is 1.49 km long. The bridge has a full width of 25.1m and a maximum span of 56m.The cover beam construction along the main line could be considered as relatively risky. There are three main structure types: T-type, M-type, and F-type, among which the 30 T-type structures constitute the majority, with each has a size of 25.11m × 3.0m × 2.4m. And the cantilever cover beam intrudes into the municipal road space beyond the range of construction project. So considering the enormous traffic flow timing, the full framing scaffolding is not feasible at the position. However, in the proposed construction the pier columns are not circular-shaped. This means greater complexity, higher cost and risk due to the uneven loading in all directions when the hoop construction method is applied. Thus, the new large cantilever assembly support is adopted for the project. This essay mainly focuses on the monitoring and analysis of such assembly support for the above-mentioned T-shaped cover beam in the project.

This kind of support system mainly contains foundation, steel

Correspondence: Qingxing Feng (501327985@qq.com).

columns, horizontal support, unloading sandboxes, beams and scissors support. Steel components are mainly made of Q235 steel. The support rods are all standard H-shaped steel. The upper chord is 588 × 300 H-type steel, the lower chord is 440 × 300 H-type steel, the connecting rod is 250×250 H-type steel, and the vertical foundation supporting member is 594 × 302 H-type steel. For more information, the foundation is connected to the column by anchor bolts of embedded parts. The middle column is connected to the C30 concrete foundation and embedded parts of the cap platform by anchor bolts, and the unloading sandbox is set between the steel columns and the beams for force transmission and unloading. The specific structure of the support is shown in Figure 1.

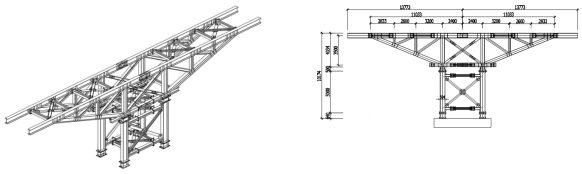

(a) Support space structure (b) Planar structure of support

Figure 1. Support structure

3. Construction monitoring and actual data analysis

3.1 Construction monitoring and forewarning

During this strain monitoring test, the monitoring positions were chosen in line with the structure position classification and the theoretical stress of the frame member. The strain monitoring was performed by using JDEBJ vibrating chord surface strain gauge, the data of which was then uploaded to the monitoring cloud through a HC-M610/4/8 wireless data acquisition instrument (Figure 2).

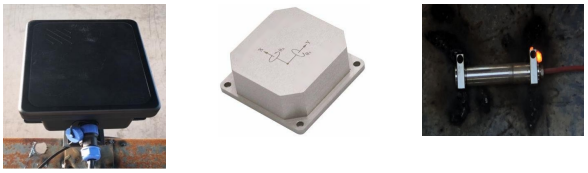

(a) Non-contact flexure tester (b) Double-axis digital inclinometer (c) Vibrating chord surface

Figure 2. Monitoring instruments

The network monitoring platform is shown in Figure 3.

It allows 24 hours uninterrupted data collection to ensure the implementation of data transmission, and it indicates timely strain situation to ensure the real-time safety of the support construction. Moreover, the IICC-NDM non-contact disturbance detector was used for displacement monitoring, and HC-B300 Double-axis digital inclinometer was used to monitor the tilt condition of the supporting frame.

Figure 3. Network monitoring platform

The specific monitoring position is shown in Figure 4. There were 30 strain monitoring stations (to monitor the safety state of some key rods under construction load two strain gauges were placed at the i-steel web and flange respectively); 6 displacement monitoring points (three deflection detectors are fixed to identify the relative positions between the monitoring positions and the measurement instruments, then to determine the displacement deformation of the supporting frame, with each instrument used to detect two displacement points); and one inclination monitoring point (placed on the central column).

(a) Product A supports (b) Product B supports

Figure 4. Layout of monitoring positions of product A and product B supports

The monitoring and early warning process is shown in Figure 5. With the construction data, the theoretical maximum strain and maximum displacement of each rod of the construction support were calculated according to the theoretical maximum construction load. The monitoring scheme (monitoring points and instruments) was determined, with the three-level warning values set, and the actual data of the support during the construction process monitored and collected throughout the day. Being under real-time monitoring, once there was a dangerous situation, the system could immediately give feedback to the construction site, adjust the construction, and then ensure construction safety, forming a closed-loop construction-monitoring chain.

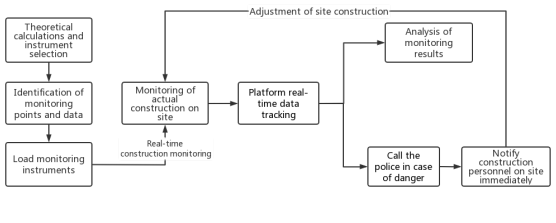

Figure 5. Monitoring and early warning flowchart

During the construction period, in order to provide early warning for the actual construction, according to the design cover beam construction load (the construction load 5 KN/m^2, the formwork load 2 KN/m^2, the concrete load 26 KN/m^2), it was considered that the support frames should all be warned within the yield load, so the theoretical maximum strain situation of the frame was calculated by the elastic theoretical calculation values of the rods (through the upper beryl beam of the support, the maximum theoretical load was evenly distributed to the two independent parallel frames), and the theoretical maximum displacement values resulting from the larger displacement positions were calculated. After taking into account the material yield strength of each member in comparison with the instability strength of the space structure, each strength meeting the requirements, a three-level warning system was proposed to guide the construction on site respectively in accordance with 110%, 120% and 130% of the theoretical maximum strain. The strain warning values of each measurement point are shown in Table 1.

Table 1. Early warning values of strain at each measuring point (strain unit: $\mu\varepsilon$)

Number	Level 1	Level 2	Level 3	Number	Level 1	Level 2	Level 3
YBA-03	915	998	1043	YBB-04	550	600	651
YBA-04D	768	845	922	YBB-05U	723	789	855
YBA-04M	768	845	922	YBB-05M	723	789	855
YBA-05	915	998	1043	YBB-06U	915	998	1043
YBA-08	550	600	651	YBB-06M	915	998	1043
YBA-09	723	789	855	YBB-11R	351	383	414
YBA-10	273	298	322	YBB-11M	351	383	414
YBA-11	620	676	732	YBB-07U	723	789	855
YBA-13	723	789	855	YBB-07M	723	789	855
YBA-14	550	600	651	YBB-08	273	298	322
YBA-12	273	298	322	YBB-09	620	676	732
YBA-16	351	383	414	YBB-10	723	789	855
YBA-15	351	383	414	YBB-12	351	383	414
YBA-02	239	261	283	YBB-13R	351	383	414
YBA-06	239	261	283	YBB-13L	351	383	414

3.2 Analysis of monitoring data

Throughout the monitoring of the whole construction process, the displacement and inclination of the actual frames were small and almost unchanged, so the main analysis was on the strain. The force transmission form on the support was similar to that of a truss structure, with two main types of the members of the support, respectively transmitting the compression force and tension force (the OA section is the reinforcement tying stage, the AB section is the concrete pouring stage, the BC section is the initial concrete setting stage and the CD section is the first tension stage of post-stressing). The full process strain trends for the two types of stressed members are shown in Figure 6.

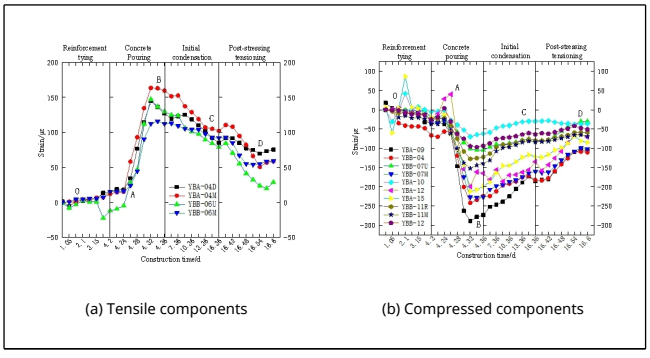

(a) Tensile components (b) Compressed components

Figure 6. Strain trend diagram of two kinds of stressed rods in the whole process

The strain trends in the whole process and the comparison with the strain data at the monitoring points show that the strain trends are the same during the whole construction process, i.e. reinforcement tying and formwork installation - concrete placement - initial concrete setting stage - primary post-stressing tensioning.

From the strain trend diagram of the whole process, we can learn that during the stage of reinforcement tying and formwork installation, as the load of the upper cover beam reinforcement and formwork slowly increased, the strain of each member of the lower support frame slowly increased as well. Although the theoretical construction load accounted for 20% of the overall load, the actual strain of the support frames was only 10% to 15% of the maximum strain. The concrete was poured after the installation of the formwork. And as the concrete was the main load of the whole cantilever cover beam, and the loading increased at a high speed, the overall strain of the lower support frames rose sharply with the pouring of concrete to the strain maximum, 289.54 $\mu\varepsilon$. But it was still within the safe range, and there was still a large gap from the theoretical strain, accounting for only 40.03% of the theoretical value. The member reaching 73.01% of the theoretical strain was the one reaching the closest.

Entering the initial concrete setting stage, the overall cover beam stiffness gradually increased due to the internal hydration of the concrete, and the load on the support was continuously released, so the stress on each member was continuously reduced, that is, the strain variables slowly fell down and dropped to 60%~75% of the maximum strain. During the stage of the primary post-stressing tensioning of the cover beam, with the post-stressing members arranged on the self-weighted tensioned side of the cover beam, and further increasing the stiffness of the cover beam, its capacity to withstand the overall self-weight was promoted as a result, and the strain continued to decrease till it reached its lowest point, approximately 50% of the maximum strain.

It can be seen that the release of the stress in the assembly support was closely linked to the continuous improvement in the stiffness of the upper cover beam. As the process continues, in the increased load section, the strain in the support frame increased with the overall load, but the actual strain, which has a large gap from the theoretical strain, basically did not exceed 75% of the theoretical maximum strain. According to the changes in the strain variables of each member, the internal stresses can be calculated, as the size of each member type was different, so the ultimate yield stress was also different 6.84%. The maximum strain and stress ratio at each measurement point are shown in Table 2. This shows that the frame member utilization was very low and the member strain surplus was still large.

Table 2. Maximum stress variable and stress ratio of each measuring point

Measurement point number	Stage maximum change strain variable ($\mu\varepsilon$)	Stress ratio (%)
YBA-04D	144.629	13.86
YBA-04M	163.48	15.66
YBB-06U	147.333	14.12
YBB-06M	115.837	11.10
YBA-09	-289.452	28.24
YBB-04	-241.991	23.50
YBB-07U	-105.09	10.25
YBB-07M	-227.754	22.22
YBA-10	-70.071	6.84
YBA-12	-199.335	19.46

YBA-15	-211.932	20.96
YBB-11R	-127.36	12.60
YBB-11M	-152.01	15.04
YBB-12	-97.025	9.60

When the concrete pouring of the upper cover beam was completed and hardening, the support was unloaded, causing the stress strain of the support to decrease. By monitoring the construction process, 10-12 days after the hardening, i.e. 15-17 days after the start of the cover beam construction (during which the first tension stage of post stressing was completed), the support strain reached a minimum of no more than 10% of the ultimate yield strain of the member, and the support was removed at this stage, which not only ensured the quality of the cover beam construction, but also improved the flow of the support and shortened the period for the bridge construction.

The monitoring data shows that the support frames are safe in practice, the actual strain is still far from the ultimate yield strength of each member, and the use of such assembled support can effectively improve the construction period of the cover beam, but the actual utilisation of each member of the support is low.

By analyzing the overall structure of the support frame, it can be found that this type of support is not a separate plane load-bearing system, but a space structure system that connects the two frames stably through transverse scissor bracing and connecting members, closely combining with the pier column below the cover beam which largely shares the bearing load, it ensures that the support frame bears a smaller load during the construction of the cover beam, thus the theoretical maximum strain of the support frame is greater than the actual strain. The finite element analysis of the spatial structure of the support was then used to verify the efficiency of each member of the frame, and will provide the theory basis for unloading mechanism of frame interaction during the concrete hardening.

4. Finite element simulation analysis

4.1 Theoretical modelling

According to the actual construction situation, member type, member size and connection form and other actual frame parameters, using the sap2000 finite element analysis software, the assembly support model was established to study the stress changes in the support frame under the theoretical construction load for each working condition and to verify the utilisation of the support frame. The assembly support frame is composed of the following 3 categories of members: upper chord members (the part where the load is placed, 588 × 300 H-beam), lower chord members (440 × 300 H-beam), web members (250 × 250 H-beam) and column members (594 × 302 H-beam). In the process of modeling, beam units were used for all types of members, with each upper chord member divided into 9 units, each web member into 16 units, each lower chord member into 3 units and each column member into 3 units. As the actual construction of each member is connected by multiple rows of high strength bolts, rigid nodes were used in the model to ensure the transfer of bending moment. The actual support at the bottom of the member is a high-strength bolt connected to the concrete pier column pre-built, so the fixed support was used. The three-dimensional calculation model is shown in Figure 7.

In the actual construction process, as the actual load of the cover beam was transferred to the main support through the upper berth and distribution beams of the support, all the theoretical loads were converted into linear loads and applied to the two main supporting frames respectively. Among them, the construction load, including manual movement, equipment placement, etc., was 11.5KN/m, the formwork load was 2.6KN/m, and the main load of the cover beam, including the theoretical weight of the concrete and the theoretical weight of the reinforcement, was 118.3KN/m. In the construction of the cover beam, the reinforcement tying stage was carried out in a homogeneous pattern, so in the modeling, the distributed loads were applied to the top chord in batches. The main load is the weight of the concrete, and the actual concrete pouring phase was divided into four stages for the safety of the construction: 1/2 weight pour from the middle to the south end; 1/2 weight pour from the middle to the north end; the other 1/2 weight pour from the middle to the south end; the other 1/2 weight pour from the middle to the north end. Therefore, when analyzing the forces at this stage in the finite element simulation, the loads were also applied according to the four stages. The stress and displacement clouds of the assembly support are shown in Figure 8.

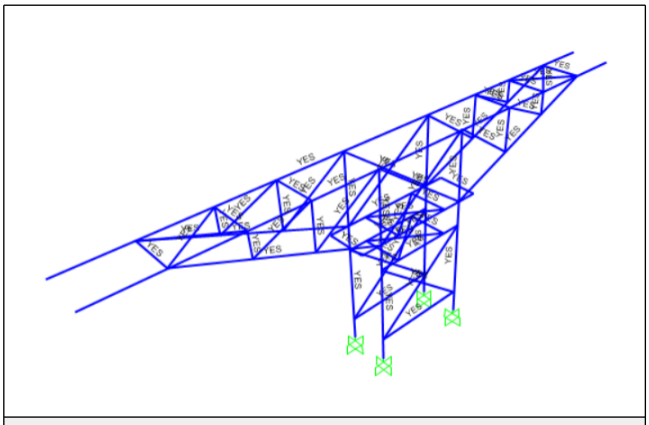

Figure 7. 3D Calculation mode

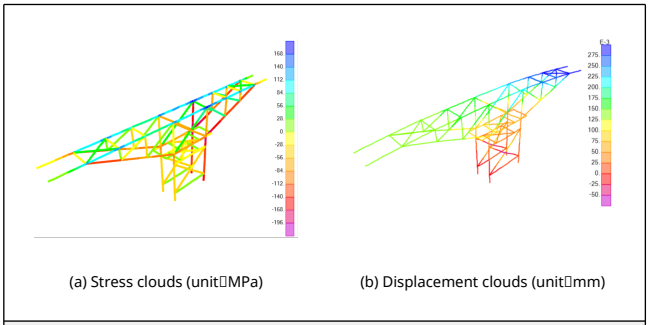

(a) Stress clouds (unit□MPa) (b) Displacement clouds (unit□mm)

Figure 8. Support nephogram

4.2 Model validation

In order to verify the reasonableness of the model, the simulated data of the two types of stressed members of the assembly support were derived and compared with the data from the actual monitoring process. The strain change process of the members is shown in Figure 9. As can be seen from Figure 7, although the simulated curve and the measured curve are different in some positions, the overall deformation development trend between the measured and simulated curves is relatively close, taking into account the actual co nstruction influence and the sensitivity of the monitoring instruments, so the model is reasonable.

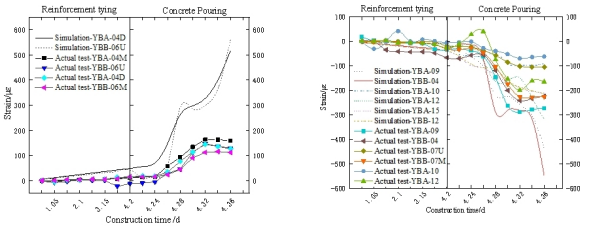

(a) Diagram of trends in tensioned components

(b) Diagram of trends in pressurized components

Figure 9. Strain change process

4.3 Analysis of calculation results

Monitoring points with continuous strain trends and low fluctuations in the measured data were selected for analysis and comparison among the various types of members in the assembly support.

4.3.1 Upper chord rod force analysis

The comparison between the actual data from the monitoring point YBB-06U at the upper chord member and the simulated data is shown in Figure 8. As can be seen from Figure 10, during the reinforcement tying stage, the simulated and measured strain data of the members increased gradually at a slow rate, but the strain variables in both were small. During the reinforcement tying stage, the maximum strain in the actual monitoring data was 11.653$\mu\varepsilon$, accounting for 8.98% of the total strain, while the maximum strain in the simulated data was 42.961$\mu\varepsilon$, accounting for 7.66% of the total strain, and the two were relatively close to each other in terms of their proportions in the total strain. During the concrete casting stage, the maximum strain in the actual monitoring data was 129.807$\mu\varepsilon$ and the maximum strain in the simulated data was 560.582$\mu\varepsilon$. Due to the actual construction conditions and the influence of the structure of the support (the fluid state of the concrete and the single-side force loading on the space structure of the support), both strains showed a trend of a slow fall after a sudden rise, followed by another sudden rise, and the maximum strains in both were less than the theoretical maximum strain of 831$\mu\varepsilon$ for the single-sided force on the member.

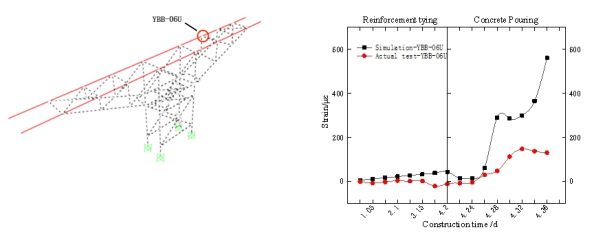

(a) Upper chord

(b) Comparison curve of actual monitoring data and simulated data at YBB-06U monitoring point

Figure 10. Strain of upper chord

4.3.2 Lower chord force analysis

The comparison between the actual monitoring data from the monitoring point YBA-09 at the lower chord and the simulated data curve is shown in Figure 11 . As can be seen from Figure 9, during the reinforcement tying stage, as in the case of the upper chord, both the simulated and measured strain data of the members gradually increased at a slow rate, but the strain variables in both were both small, and as the construction stage reached the concrete pouring stage, the main construction load increased at a faster rate, the strain variables in both increased significantly, and the strain variables in both were very close to each other, and the strain convergence trend in both were more consistent. During the reinforcement tying stage, the maximum strain in the actual monitoring data was -33.479$\mu\varepsilon$, accounting for 12.24% of the total strain, and the maximum strain in the simulated data was -33.655$\mu\varepsilon$, accounting for 7.74% of the total strain. During the concrete placement phase, the maximum strain in the actual monitoring data was -273.435 $\mu\varepsilon$ and the maximum strain in the simulated data was -435.145 $\mu\varepsilon$, both maximum strains were less than the theoretical maximum strain of -657$\mu\varepsilon$ in the members.

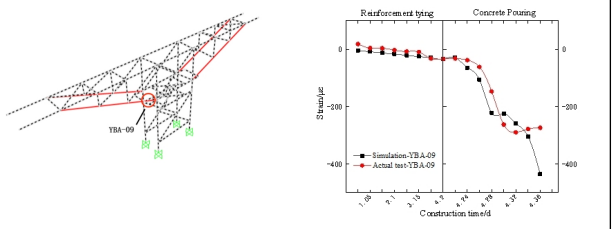

(a) Lower chord

(b) Comparison curve of actual monitoring data and simulated data at YBA-09 monitoring point

Figure 11. Strain of lower chord

4.3.3 web bar force analysis

The comparison curve between the actual monitoring data and the simulated data for the monitoring point YBA-10 at the web is shown in Figure 12. As can be seen from Figure 10, during the reinforcement tying stage, unlike the situations of the upper and lower chords, the simulated data of the member strain still increased gradually at a slow rate, while the actual measured data had a tensile and compressive transformation. The reason was that during the actual construction process, the reinforcement loads were not actually tied evenly as in the ideal situation, resulting in positive and negative fluctuations of the web strain caused by the single-sided force loading on the assembly support. But the overall tendency was still consistent with the simulated result, and both strains were smaller at this stage. The final strain variables were small, and as the construction phase reached the concrete pouring phase, the main construction loads increased at a faster rate, and both strain variables increased significantly, with the trends of strain convergence in both the same. During the reinforcement tying stage, the maximum strain in the actual monitoring data was -4.974$\mu\varepsilon$, accounting for 7.96% of the total strain, while that in the simulated data was -12.65$\mu\varepsilon$, accounting for 13.61% of the total strain. During the concrete placement phase, the maximum strain in the actual monitoring data was -62.495$\mu\varepsilon$ and that in the simulated data was -91.602$\mu\varepsilon$, both of which were less than the theoretical maximum strain of -248$\mu\varepsilon$ in the members.

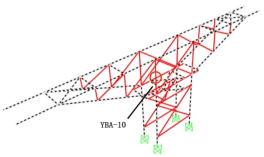

(a) Web bar

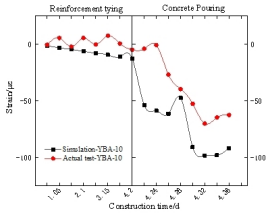

(b) Comparison curve of actual monitoring data and simulated data at YBA-10 monitoring point

Figure 12. Strain of web bar

4.3.4 Column bars rod force analysis

The column member, as the main load-bearing structure of the assembly support, has the largest dimensions and a clear strain trend. The comparison between the actual monitoring data from the monitoring point YBA-15 at the column member and the simulated data curve is shown in Figure 13. As can be seen from Figure 11, during the reinforcement tying phase, as in the case of the web member, the simulated strain data of the member still increased gradually at a slow rate, while the actual measured data had a tensile and compressive transformation. The reasons was assumed to be the same as in the web member, and the overall tendency is still consistent with the simulated result. The final strain variables were smaller at this stage, and as the construction phase reached the concrete pouring phase, the main construction load increased at a faster rate, and both strain variables increased significantly. Unlike in the other members, the growth curve of the concrete casting section of the column member kept smooth and steady until the maximum strain was reached, and the trends of strain convergence in both were the same. During the reinforcement tying stage, the maximum strain in the actual monitoring data was -18.745με, accounting for 9.3% of the total strain, while the maximum strain in the simulated data was -39.995με, accounting for 18.92% of the total strain. During the concrete placement phase, the maximum strain of the actual monitoring data was -198.569με and the maximum strain of the simulated data was -211.359με, with an error of 6.05%. Both were less than the theoretical maximum strain of -319με for the members.

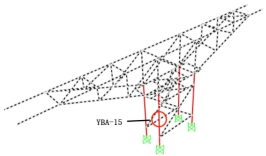

(a) Column members

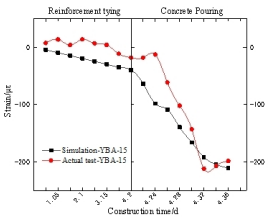

(b) Comparison curve of actual monitoring data and simulated data at YBA-15 monitoring point

Figure 13. Strain of column pole

The above analysis shows that the simulated strains of the model are consistent with the actual strains, but the actual monitoring situation was influenced by many factors at the site (construction conditions, construction sequence, construction equipment, etc.), and the actual strains may fluctuate significantly, but the overall trend is relatively stable. Compared to the simulated strain, the actual maximum strain is small, not exceeding 62.24% of the theoretical maximum strain of the member, while the simulated data does not exceed 66.26% of the theoretical maximum strain of the member. In the simulation modeling, the spatial connection mode of the assembly support was not taken into consideration. The spatial structure of the assembly support was simplified as two independent plane supporting frames. And the construction load was viewed as distributed load, with each plane supporting frame bearing 1/2 of the load. While in the actual construction situation, The special connection between the two frames and their hoop joints with the pier columns below lead to the decrease of the member strain, much less than the theoretical maximum strain, so there is still more space to reach the ultimate yield strength of the member itself, and no instability is generated. Therefore, the safety of the assembly support in actual construction is guaranteed, and the utilization rate of the member is low, and the member can be optimized.

5. Conclusions

This study combines engineering examples to investigate the assembly support for a large cantilever poststressed cover beam in the Pengbu Interchange Reconstruction Project in Hangzhou, using a combination of real-time monitoring of actual construction and finite element analysis of the simulation modeling, resulting in the following conclusions:

(1) Based on the clear process of the real-time monitoring in a closed-loop chain and the information changes in the support frames during the whole construction process, the three-stage warning mechanism on the construction process ensured the safety of the support frames during the whole construction, and confirmed the safety of such assembly support for the large cantilever poststressed cover beam. And this can provide reference for such monitoring projects.

(2) The strains of the support frames during the whole-process construction were monitored and the whole-process strain trend diagram was derived. The analysis of the whole-process strain trend enables a clear view of the changing trend of the strains within the support frames in different phases of the process, and it was proposed that the best time for the flow of the frames is when the stress ratio was reduced to 10% on the basis of the calculation of the stress ratio of each member. This provides a theoretical basis for the future use of such assembled frames.

(3) By comparing the finite element simulation data with the actual monitoring data analysis, the actual strain was overall smaller than the simulated strain, and the member utilization rate of the assembly support is low. The study provides reference for the optimization of the member as well as the structural system of such assembled support frames in the future. The further analysis of the future unloading process during concrete hardening and the study on reasonable flow timing will provide reference for the study of the dismantling sequence of the frame during flow.

References

[1] Guo Z., Li H., Zhou Y. Research on the application of safety technology for the construction of fastening scaffolding in housing construction. Anhui Arrchitecture, 26(3):41, 2019.

[2] Fang B., Yu H., Ma K. et al. Research on the bearing mechanism of tall formwork support system for coal tower project. Structural Engineer, 36(5):173, 2020.

[3] Zhou G., Wan J., You G. et al. Analysis of the construction process of the open and closed roof of Hangzhou Olympic Sports Tennis Center. Space Structure, 27(2):70, 2021.

[4] Zhang Z., Chen X., Lin B., et al. Study on the stability of axial compression under scaffold riser casing joint. Journal of Building Structures, 43(1):228, 2022.

[5] Zhang L., Liu C., Xu X., et al. Finite element analysis of X-pillar and ring-beam fastener-type full-span braced scaffolding for cooling towers. Special Structures, 35(6):21, 2018.

[6] Liu F., Li W.J., Xu C.C. Application of coiled buckle scaffolding in the support system of double curved large span cast-in-place box beam. China Building Metal Structure, No. 484(4):59, 2022.

[7] Wu X., Han J., Zhao K. Analysis of mechanical characteristics of cast-in-place large-span retentions of main girders of wide-span cable-stayed bridges. Spatial Structures, 24(2):86, 2018.

[8] Lin Y.. Analysis of the construction process of the main steel structure of Lusail Stadium. Special Structures, 37(4):116, 2020.

[9] Wang J. Technical and safety research of tie rod suspension frame system in assembled buildings. China Building Metal Structure, No. 484(4):26, 2022.

[10] Wang H., Tang X. Analysis of unloading process of structural support frame of No.2 bridge on Yuhai West Road, Qianwan New Area, Ningbo. China Building Metal Structure, No. 466(10):113, 2020.

[11] Yan X., Wang S., Gong Z., et al. Construction technology of cast-in-place box culvert bracket erection and pre-pressure in limited space under railway. Engineering Quality, 39(9):35, 2021.

[12] Li M.R., Zhang Q.M. Research on construction monitoring scheme of Jiangsu Yunjingtai project. Anhui Architecture, 28(10):215, 2021.

[13] Wu Jun. Exploration of automatic monitoring system for building settlement and tilt. Anhui Architecture, 27(2):126, 2020.

[14] Ye B. Application of socket-type coiled buckle bracing frame for building construction. Engineering Quality, 39(10):57, 2021.

[15] Huang Y., Zhang L., Zuo Z., et al. Real-time monitoring-based control technology for integral steel platform mouldings. Spatial Structures, 27(2):83, 2021.

[16] Wu Y., Yin S., Yin Y. Simulation analysis and construction monitoring of pre-stressed pipe truss structure construction for large span dry coal sheds. Space Structure, 27(1):37, 2021.